International Journal of Metallurgical Engineering 2015, 4(1): 12-23
DOI: 10.5923/j.ijmee.20150401.03

Effect of Annealing on Microstructure and Mechanical Behaviour of Cold Rolled Low C, High Mn TWIP Steel

N. K. Tewary, S. K. Ghosh*, S. Chatterjee

Department of Metallurgy & Materials Engineering, Indian Institute of Engineering Science and Technology, Howrah, India

Abstract In the present study, 10% and 30% cold rolled Fe-21Mn-3Si-3Al-0.06C TWIP steels have been annealed in the temperature range of 600-900 ℃ for a short duration of 5 min. Optical and TEM microstructures reveal dislocations, micro-shear bands, deformation twins as well as interaction of dislocations and twins when deformed 10-30% by cold rolling. After annealing in the temperature range of 600-800 ℃, cold deformed austenite structures undergo recovery, whereas recystallisation occurs at 900 ℃. It is noticed that the hardness, yield strength and tensile strength of the specimens increase whereas percentage elongation decreases as the amount of cold rolling reduction increases. Tensile test results show improvement in ductility and decrease in tensile strength of cold rolled samples subjected to annealing at 600 ℃. 30% cold rolling and annealing can be considered as an effective method to obtain submicron grain with an attractive combination of strength and ductility.

Keywords Steel, Cold rolling, Annealing, Microstructure, Mechanical properties

1. Introduction

In the current century, advanced automobile researchers pay much attention on light weight vehicle which boosts fuel economy along with the reduction in emission of greenhouse gases. Substantial weight savings is possible only through extensive research on advanced high strength steel (AHSS). In order to fulfil this optimal combination, a variety of Advanced High Strength Steels (AHSS) has been developed such as Dual Phase (DP), Complex Phase (CP), Transformation Induced Plasticity (TRIP) and most recently, Twinning Induced Plasticity (TWIP) steels. Among the wide variety of recently developed steels, TWIP steel with light weight and high tensile strength along with adequate formability has become favourable to researchers due to its low stacking fault energy (SFE) and twinning effect [1]. High manganese TWIP steels have a good potential to manufacture such as structural reinforcements and energy absorption parts in the automotive industry.

TWIP steel possesses a fully austenitic structure at room temperature mainly due to its high content of Mn which can be a range up to 17-30 wt% [2]. Below 17 wt%, it can't suppress $\gamma \rightarrow \alpha$ transformation [3]. Mn is not only an effective austenite stabiliser but also an element which increases SFE of TWIP steels. Apart from Mn, other ingredients such as C, Si, Al etc are added to this type of steel. In general, addition of Al increases SFE and strongly suppress $\gamma \rightarrow \alpha$ transformation so that the formation of deformation twin is favoured. In contrast, Si decreases SFE and sustains $\gamma \rightarrow \alpha$ transformation during cooling and deformation.

The explanation for high strength and ductility of TWIP steels is still controversial. Some authors quantify this due to dynamic strain aging (DSA) mechanism [4], interpreted as the interaction between C–Mn bonds and mobile dislocations and some other justify it by its twinning mechanism [5]. During plastic deformation, deformation twinning plays a key role for this class of materials and the deformation mechanisms are closely related to the SFE of the austenitic phase. As the strain increases, the occurrence of twins reduces the mean free path of dislocations [6].

Cold working is generally applied to metals and alloys having high ductility [7]. The dislocation density as well as deformation twins increase with increasing amount of cold deformation in TWIP steel which results in improvement in strength achieved by dislocation-dislocation interaction as well as the interaction of dislocations with twin boundaries. However, greater deformation exhibits lowering ductility which can be improved by subsequent recovery treatment. It has been found that nano-scale mechanical twins have a thermal stability during recovery treatment [8].

The purpose of this paper is to get a comprehensive understanding of the extensive microstructural observation after recovery and partial recrystallisation. These include studies of the present investigated steel in primarily cold rolled and annealed conditions. Several characteristics

* Corresponding author:
skghosh@metal.iiests.ac.in (S. K. Ghosh)
Published online at http://journal.sapub.org/ijmee

features of recovery and recrystallisation are described. Attempt has been made to get a correlation between processing-microstructure and mechanical property and finally the properties of the developed steel have been compared with high strength automotive steels. The present study also pays attention to the stability of mechanical twins at elevated temperature.

2. Experimental

2.1. Materials Preparation

A 25 kVA air induction furnace was used to manufacture the investigated steel with the chemical composition as listed in Table 1. After cropping the top section of the ingot containing shrinkage/pipes, the remaining ingot of 200 mm × 50 mm × 50 mm size was hot forged down to 16 mm thick slab, which was further soaked at 1200°C for 40 minutes and subsequently rolled down to 8 mm thick plate in three passes with the finish rolling temperature (FRT) of 800°C. The hot rolled and air cooled (AC) samples were solution treated at 1040°C for 1h to remove any inhomogeneities followed by water quenching to room temperature. Subsequently, the above solution treated samples were cold rolled by 10-30% reduction in thickness in several passes using a laboratory scale rolling mill. These samples were then suitably annealed in the temperature range of 600℃ to 900℃ for a fixed duration of 5 minutes followed by water quenching.

Table 1. Chemical composition of the investigated TWIP steel (wt. %)

C	Mn	Si	Al	S	P	Fe
0.06	21.5	3.11	3.56	0.009	0.008	Bal.

2.2. Experimental Procedures

The Vickers hardness (HV) values of the samples after cold deformation and annealing treatments were evaluated in a Vickers hardness tester (Leica-VMHT) using 2 kg load for 20s dwelling time and were shown in Table 2. ASTM E8M standard was followed to prepare sub-size tensile specimens having gauge length of 25 mm and the tests were carried out in an Instron 5900R testing machine using an extensometer with a crosshead speed of 0.5 mm/min. At least three specimens were tested and the average values were reported in Table 3. Both cold rolled and annealed samples were prepared by the conventional metallographic techniques and etched with 10% nital solution to reveal the microstructure of the specimens under the optical microscope (Carl Zeiss, AXIOVERT 40 MAT). For transmission electron microscopy, typical 3 mm diameter thin (~ 80 μm thick) discs were subjected to twin jet electro-polishing using a mixture of electrolyte of 90% acetic acid and 10% perchloric acid at a temperature of about 10-12°C. The thin electron transparent samples were examined in a high resolution transmission electron microscope (HRTEM) (Tecnai G^2) at 200 kV operating voltage.

Table 2. Hardness values of different cold deformed specimens subjected to annealing at various temperatures

Sample ID	Hardness (HV)				
	Before annealing	600 ℃	700 ℃	800 ℃	900 ℃
10% CD	244 ±5	196 ±5	189 ±3	185 ±3	169 ±3
30% CD	320 ±3	314 ±4	304 ±4	291 ±3	182 ±3

ID: Identification, CD: Cold deformation

Table 3. Tensile test results of different samples

Processing condition	YS (MPa)	UTS (MPa)	YR	TEL (%)	Toughness (MPa)
HR+AC (0% CD)	275	480	0.57	55.8	252.77
HR+AC + 10% CD	744	865	0.86	34.1	254.8
HR+AC+ 30% CD	837	926	0.90	29.1	207.7
HR+AC+ 10% CD + Annealed (600 ℃, 5 min.)	493	662	0.46	48.2	264.5
HR+AC+ 30% CD + Annealed (600 ℃, 5 min.)	654	812	0.81	43.3	297.4

3. Results

3.1. Microstructure Evolution

Figure 1(a) shows the optical micrograph of hot rolled - air cooled sample depicting equiaxed austenite grains with some annealing twins (AT). Ferrite phase of brighter contrast is apparent along the grain boundary of austenite grain. Some inhomogenities /intergranular carbide precipitates may be segregated with the above ferrite phase. Similar types of microstructural constituents were reported earlier in case of dual phase TWIP steel [9]. Figure 1(b) shows the optical micrograph of hot rolled and solution treated (1040°C, 1h) specimen revealing fully austenitic structure with annealing twins. It may be mentioned that the above solution treatment is essential to remove the heterogeneities associated with the hot rolling operation. Figure 1(c) shows the optical microstructure of 10% cold deformed (CD) sample which exhibit both annealing twin (AT) and deformation twins (DT). 30% cold deformed sample reveals predominantly higher amount of deformation twins (Fig. 1(d)). In this context, it is obvious that increasing amount of deformation leads to more deformation twins in structure. It is important to note that deformation/mechanical twins are finer compared to annealing twins and they are activated within grains and are blocked by grain boundaries.

Figures 2(a) to (d) show the optical micrographs of hot rolled - air cooled and 10% cold deformed samples after annealing at 600℃ to 900℃ for 5 minutes. The occurrence of recrystallised grains is strongly dependent on temperature. Annealing at 900℃ leads to recrystallisation of the deformed austenite grains. The regions with higher

deformation have high density of dislocation and twins are almost identical from adjacent regions during recovery 600 ℃ to 800 ℃. It is obvious that while at lower temperature regime (600 ℃-800 ℃) recovery has taken place (Fig. 2(a) - (c)), recrystallisation is perceptible at higher temperture (900°C) (Fig. 2(d)). Presence of nano-scale mechanical twin in the temperature range of 600°C- 900°C indicates its thermal stability during annealing treatment.

Figures 3(a) to (f) show the TEM micrographs of 10% cold rolled specimen subjected to annealing at 900 ℃ for 5 minutes. Figure 3(a) exhibits commencement of recovery with some evidence of formation of parallel microshear bands i.e., narrow sheet-like regions of concentrated plastic deformation, which may be induced during dislocation slip [10]. Figure 3(b) reveals the dislocation cell structure indicating progress of recovery. Grain boundaries emit bundles of stacking faults as shown in Fig. 3(c). Figure 3(d) reveals deformation twins of few nanometer (<100 nm) thickness. Annealing at 900 ℃ leads to the formation of recovered grain with annealing twins (Fig. 3(e)). Figure 3(f) reveals partially recrystallised submicron grain along the deformed austenite grain boundary. Thus, the detailed TEM investigation coorborates the microsrtuctural observation in optical microscope.

Figures 4(a) to (d) reveal optical micrographs of hot rolled - air cooled and 30% cold deformed samples subjected to annealing in the temperature range of 600 ℃ - 900 ℃ for 5 minutes showing characteristics features developed during annealing. Annealing in the temperature range of 600°C-800°C primarily indicates recovery, whereas the same at 900 ℃ leads to recrystallisation of the deformed austenite grains. In Fig. 4(d), it has been noticed that the recrystallised area of 30% CD and annealed at 900 ℃ is more than that shown in Fig. 2(d) for 10% CD and annealed at 900 ℃. Such kind of observation may be related with the fact of higher degree of recrytallisation (Fig. 4(d)) as the driving force associated with 30% deformation is higher [11]. In Figs. 4(a) to (d), it can be observed that mechanical twins which has been formed by cold rolling at room temperature are stable up to the perceptible recrystallisation temperature (900 ℃).

Figures 5(a) to (f) show the TEM micrographs of 30% cold rolled specimen subjected to annealing at 900 ℃ for 5 minutes. Annealing at 900 ℃ leads to partial recrystallisation of the deformed austenite grains and thereby submicron austenite grains are observed in the microstructure (Fig. 5(a)). Figure 5(b) shows dislocation pileup along the grain boundary indicating recovery phenomenon. Grain boundaries emit bundles of wider stacking faults [12] as shown in Fig. 5(c). Figure 5(e) confirms twinned spot (indicated by arrow) in the selected area electron diffraction (SAED) pattern taken from the denoted circular area shown in Fig. 5(d). Figure 5(f) reveals twin-stacking faults (SFs) interaction. It is also apparent that the thickness of mechanical twins are of a few tens of nanometer. The presence of twins and stacking faults indicate the progress of recrystallisation [13] for 30% CD samples subjected to annealing at 900 ℃ for 5 minutes. However, strain free fully recrystallised grain structure may be expected to be formed at higher annealing temperature or at higher duration than 5 minutes at 900°C.

Figure 6 shows the schematic illustration of progressive twin density obtained after cold rolling and it also reveals submicron grain associated with deformation twins after annealing.

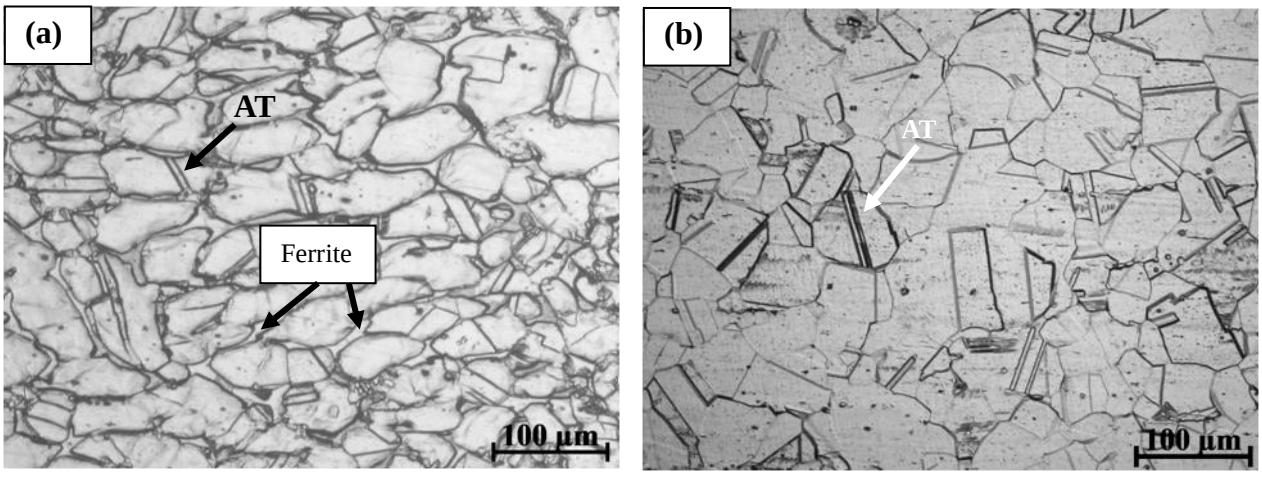

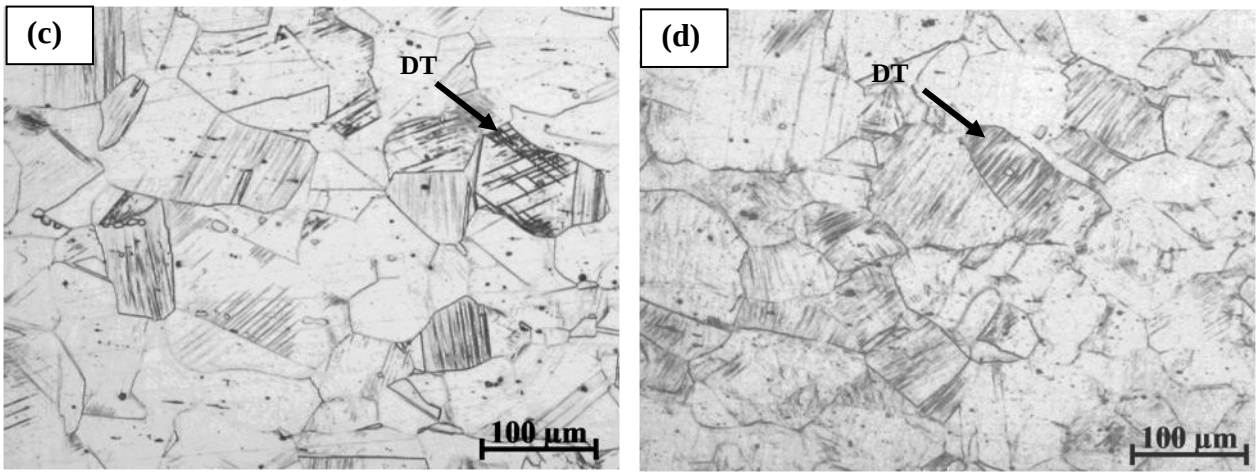

Figure 1. Optical micrograph of (a) hot rolled – air cooled with 800°C FRT, (b) hot rolled and solution treated (1040°C, 1 h) specimen, (c) 10% cold deformed sample shows annealing twin (AT) and deformation twins (DT) and (d) 30% cold deformed sample reveals higher amount of deformation twin

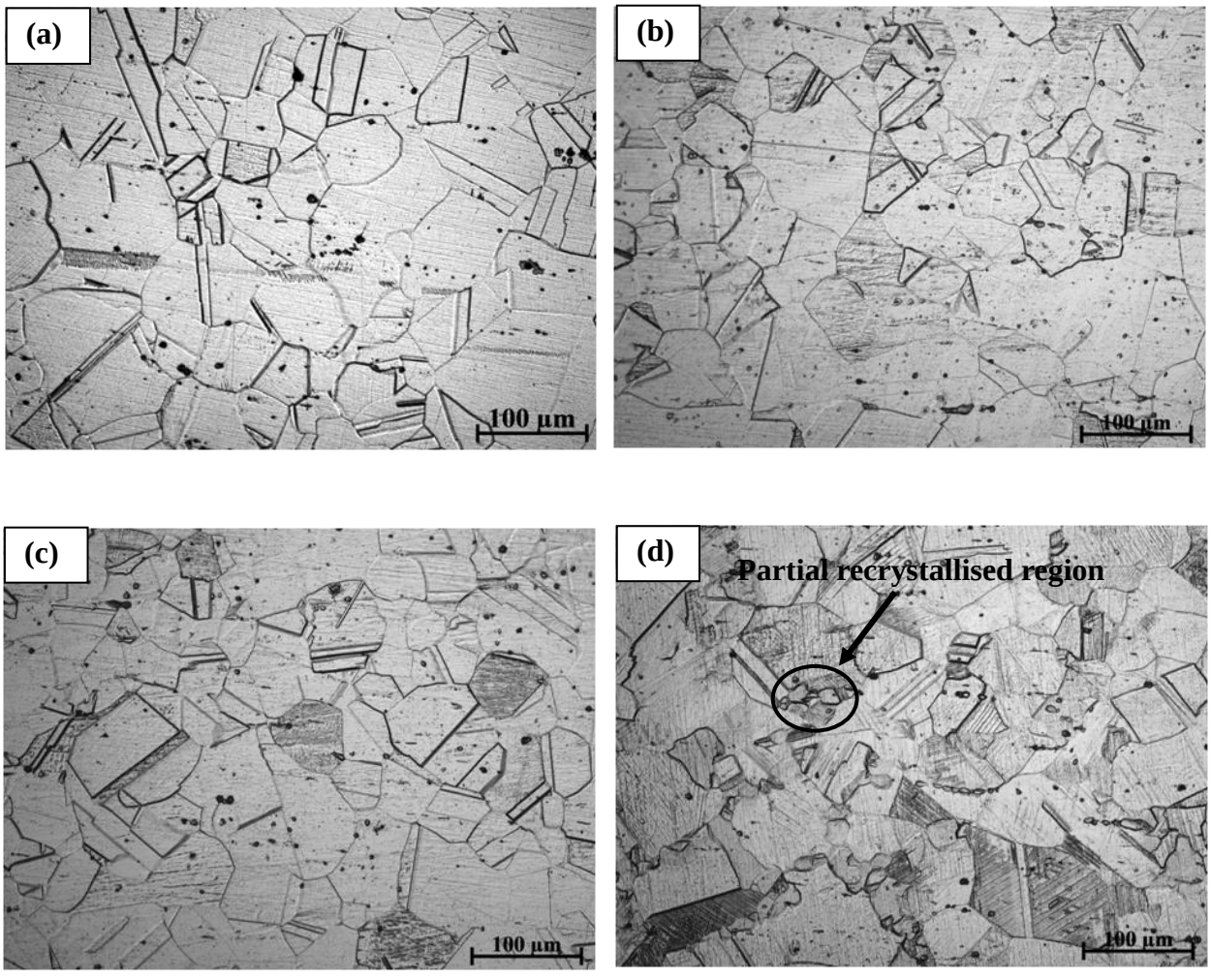

Figure 2. Optical micrograph of hot rolled - air cooled and 10% cold deformed samples subjected to annealing for 5 minutes at (a) 600 ℃, (b) 700 ℃, (c) 800 ℃ and (d) 900 ℃

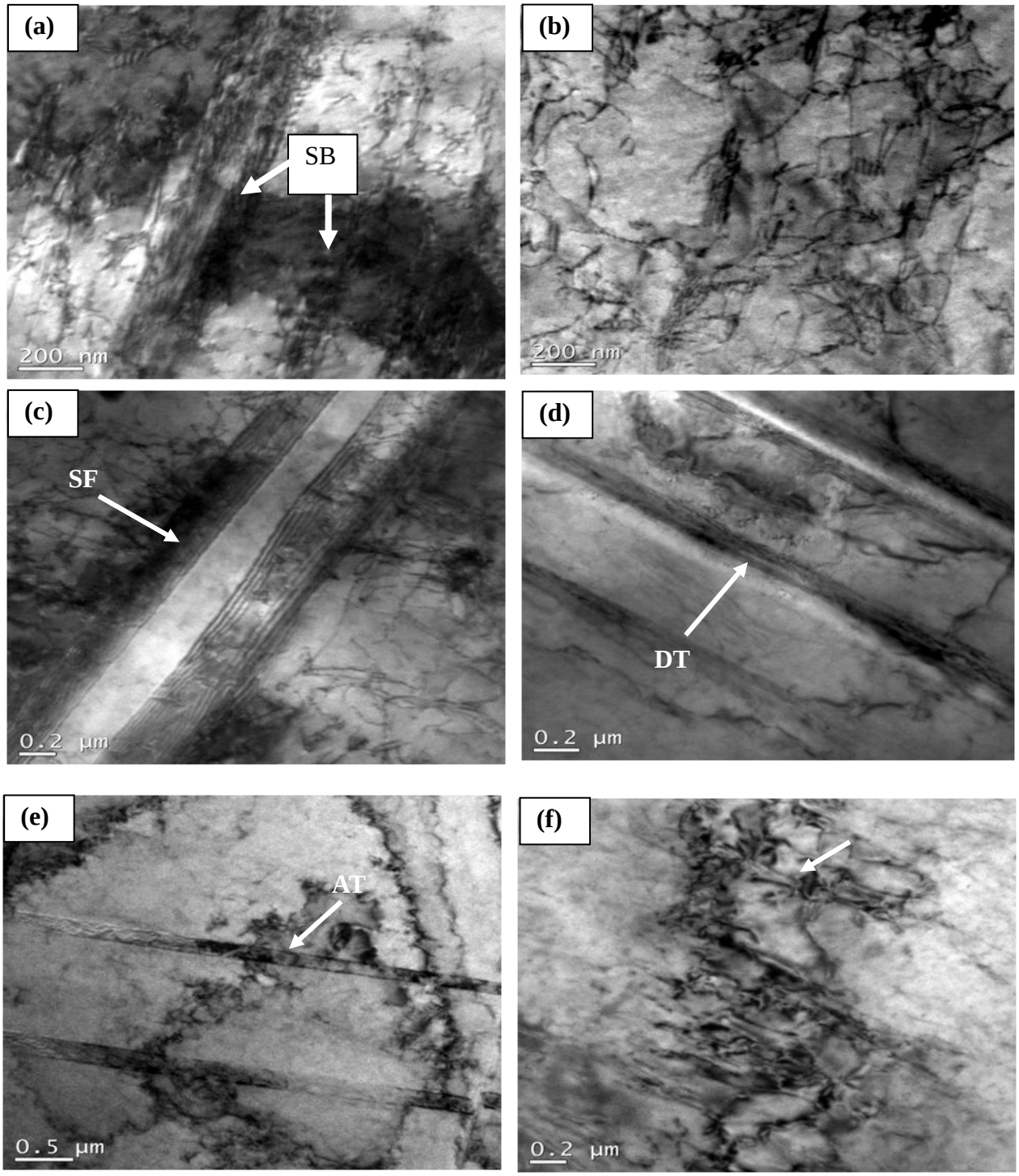

Figure 3. TEM bright field (BF) micrograph of 10% cold rolled and annealed (900 ℃, 5 min.) specimen showing (a) onset of recovery, (b) dislocation cell structure indicating progress of recovery, (c) twin-stacking faults (SFs) interaction, (d) deformation twins (DT), (e) recovered cellular region with annealing twins (AT) and (f) partially recrystallised submicron grain (denoted by arrow) along the deformed austenite grain boundary

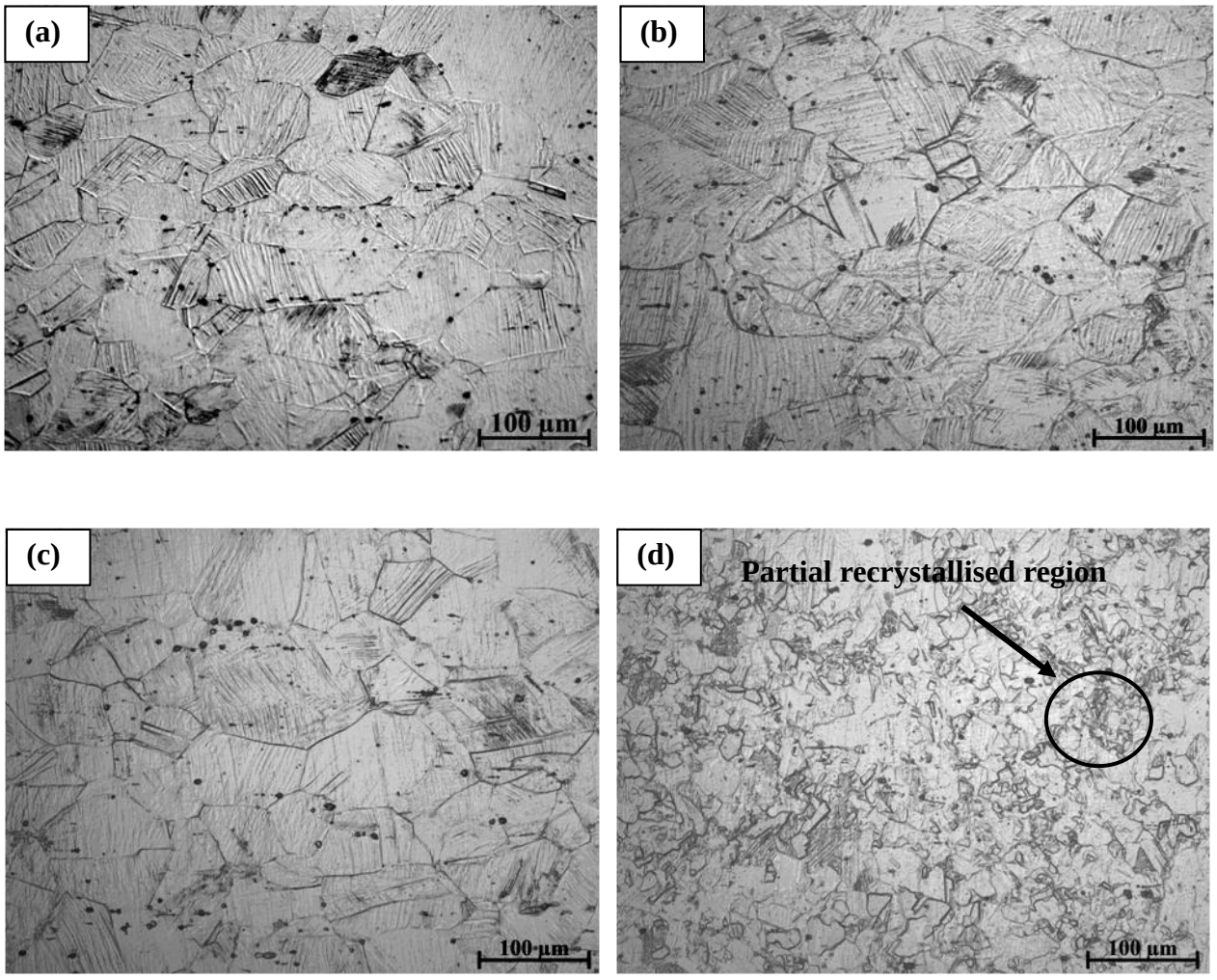

Figure 4. Optical micrograph of hot rolled - air cooled and 30% cold deformed samples subjected to annealing for 5 minutes at (a) 600 ℃, (b) 700 ℃, (c) 800 ℃ and (d) 900 ℃

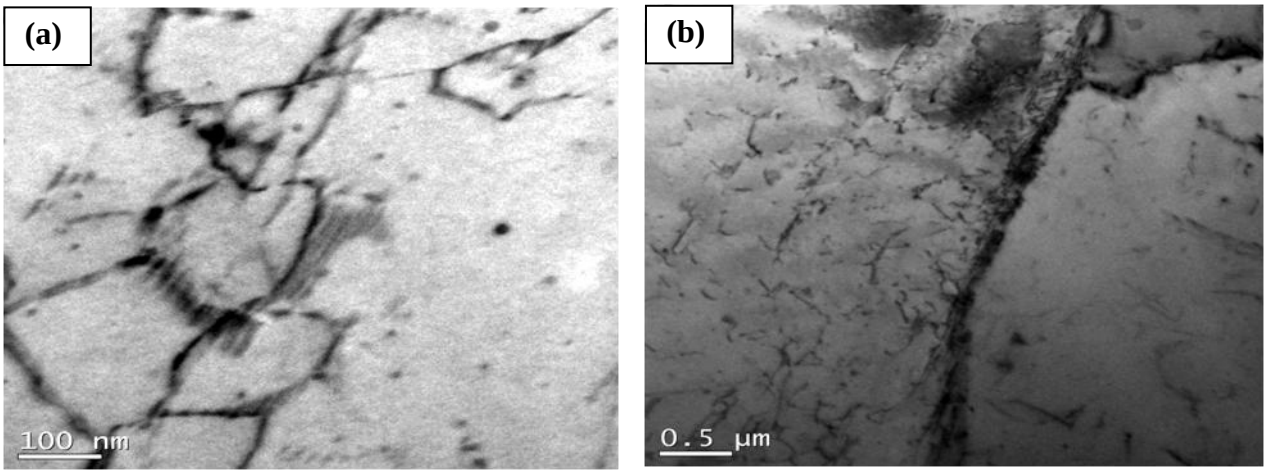

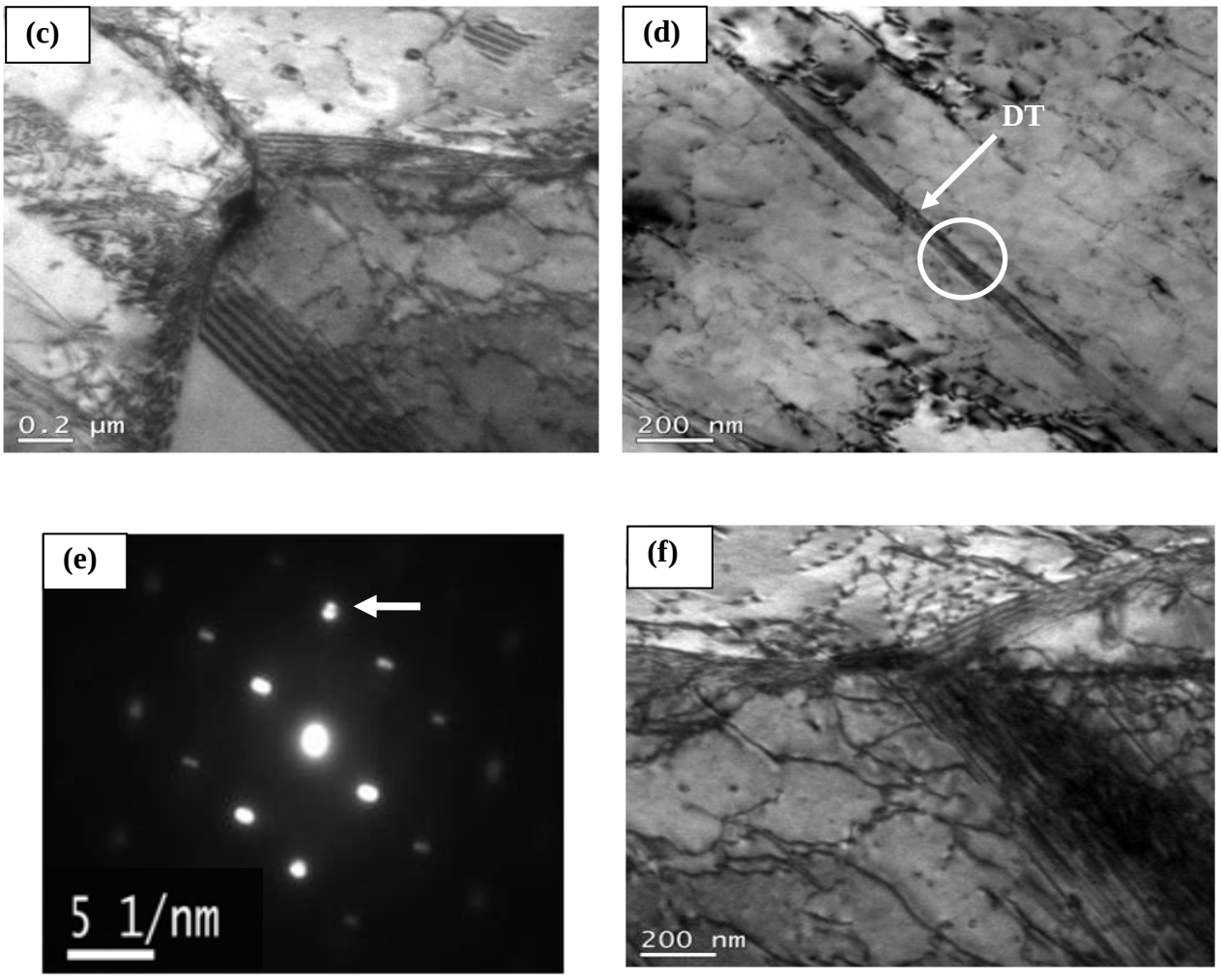

Figure 5. TEM BF micrograph of 30% cold rolled and annealed (900 ℃, 5 min.) specimen showing (a) partially recrystallised submicron austenite grain, (b) dislocation pile up along the austenite grain boundary, (c) stacking faults (SFs), (d) deformation twin (DT), (e) SAED pattern with the twinned spot (denoted by arrow) confirming DT and (f) twin-stacking faults (SFs) interaction at 900 ℃

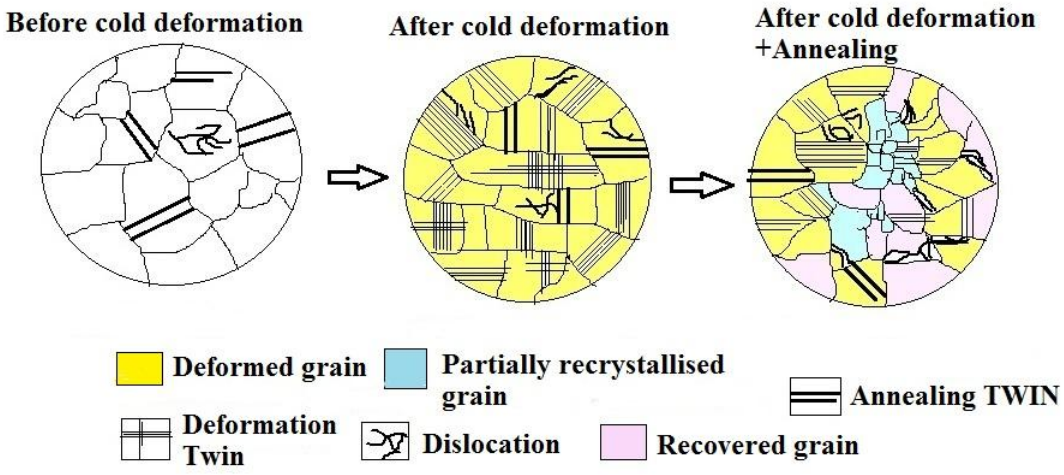

Figure 6. Schematic illustration showing microstructural changes before and after cold rolling and annealing

3.2. Mechanical Property

3.2.1. Hardness

Table 2 and Fig. 7 show Vickers hardness values (HV) of 10% and 30% cold deformed samples before and after annealing treatment. It has been already noticed from previously described microstructural evolution that by annealing treatments at 600 ℃ to 900 ℃ for 5 minutes recovery and partial recrystallisation occur and thereby hardness values decrease with the increase of annealing temperature. The slope of the hardness curve decreases prominently after annealing at 700 ℃ and it is more predominant in 30% CD than 10% CD samples. It can be mentioned that recovery is more prominent than recrystallisation within the temperature range of 600 ℃ to 700 ℃. At 900 ℃, the hardness values are minimum for both 10% and 30% CD samples. This can be attributed to the fact that the softening is now dominated by recrystallisation instead of recovery.

3.2.2. Tensile Results

Table 3 summarises the tensile test results of hot rolled and air cooled specimens as well as in different cold deformed conditions before and after annealing treatments. It is noticed that good combination of high tensile strength and total elongation (TEL) can be achieved by cold rolling. It is clearly observed that the yield strength (YS) and ultimate tensile strength (UTS) of the specimens increase with the increasing amount of cold deformation which is in line with the earlier reports [14]. The increasing trend of strength properties has been found to be more pronounced when the specimen was given 30% cold deformation. This type of behaviour is attributed to the strain hardening phenomenon owing to interaction among dislocations and twins generated by cold deformation [15]. After recovery during annealing at 600 ℃ for 5 minutes, the ductility has been improved (48% for 10% CD and 43% for 30% CD specimens) with decrease in tensile strength (662 MPa for 10% CD and 812 MPa for 30% CD specimens). In the mean time, the deformation twins induced by cold rolling remain during annealing at 600°C and expected to overcome the loss of strength after annealing.

Figure 8 shows comparison of results obtained from the tensile testing of the experimental steels. Figures 8(a) and (b) show that 30% cold deformed sample has the maximum YS and UTS among all samples. It is evident that with the increase in percentage of cold deformation strength value increases. Figure 8(c) reveals that after annealing at 600 ℃ for 5 minutes the ductility is restored or increasing. Figure 8(d) indicates that the maximum toughness is achieved in case of 30 % cold rolled and annealed (600 ℃ for 5 min.) specimen. Low yield ratio (YR) (0.46-0.81) (Table 3) along with high strength, obtained after cold deformation and annealing, also ensures high energy absorption capacity of the steel (toughness) which improves the reliability of the steel during operation in service.

A careful comparison of these results reveals that a favourable combination of strength and ductility could be achieved due to the formation of recovered grain and deformed area obtained after annealing at 600°C. These results are in agreement with the fact that the cold-worked and annealed specimens, with partially recrystallised microstructures could retain excellent ductility and strength [16].

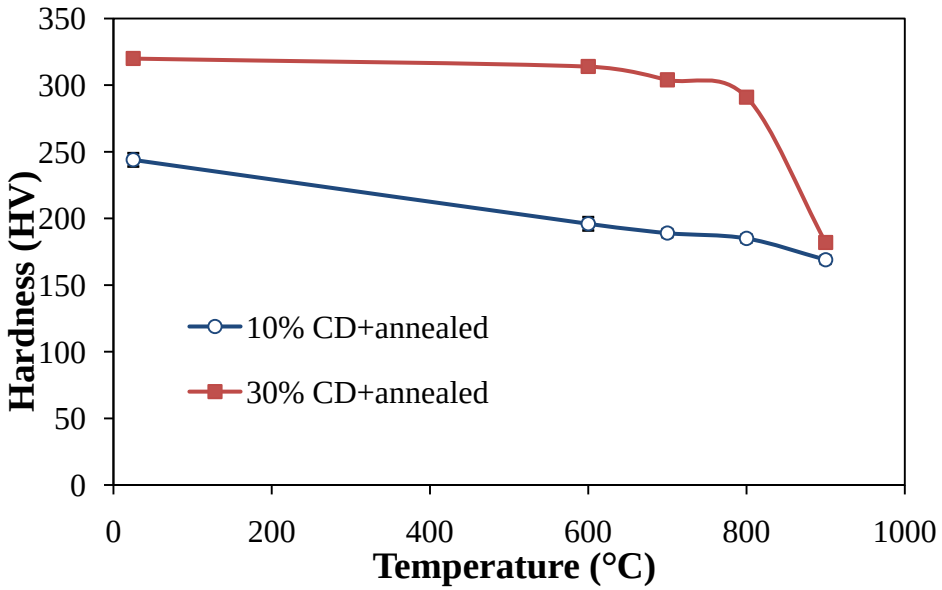

Figure 7. Hardness versus temperature plots of 10% and 30% cold deformed specimens subjected to annealing at different temperatures for 5 minutes

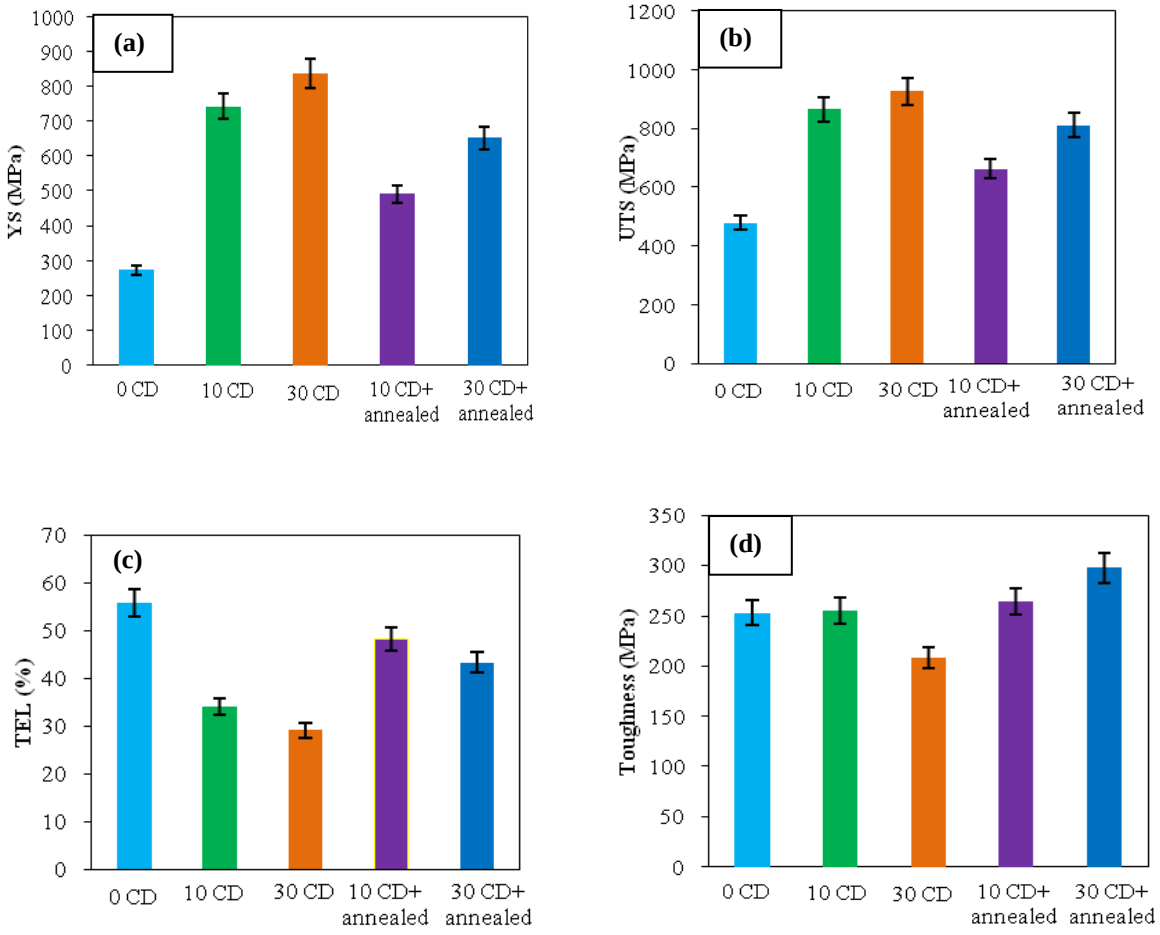

Figure 8. Comparison of tensile test results (a) Yield Strength (YS), (b) Ultimate Tensile Strength (UTS), (c) Total elongation (TEL) and (d) Toughness of cold deformed and annealed (600 ℃, 5 min.) samples

4. Discussion

The microstructure after hot rolling consists of austenite and ferrite (Fig. 1(a)) which have been elongated through hot rolling. This duplex microstructure is plausibly caused by Al, which stabilised the ferrite at the high temperature at which the hot rolling was performed. Mn segregation frequently occurs for high Mn containing steel and has an influence on the microstructural evolution [17]. Mn is an austenite stabiliser and, therefore, the ferrite could preferentially form in a Mn-lean region.

The optical micrographs of 10% and 30% cold deformed samples comprise fully austenitic structure with annealing and deformation twins. It is evident that density of deformation twin increases significantly with the increasing degree of deformation (Fig. 1). It is important to note that the present steel which has been deformed under cold rolling at room temperature, a part of the energy of deformation is stored as the increase in the dislocation density and the balance is consumed in forming deformation twins (Fig. 3). It is known that recovery of deformed steel is a process that takes place prior to recrystallisation during annealing and it is generally used to recover the properties up to some satisfactory level which dropped during deformation [18]. During recovery, dislocations annihilate or rearrange themselves in configurations of lower energy [19]. After annealing in the lower temperature range of 600-800 ℃, microstructure comprises a mixture of twinned deformed grains and dislocation-free recovered grains for both 10% and 30% CD samples. Annealing at higher temperature of 900 ℃ leads to the formation of a mixture of partially recrystallised and deformed areas with imperfections like stacking faults, annealing and deformation twins (Figs. 3 and 5). The optical micrographs presented in Figs. 2(d) and 4(d) reveal that recrystallisation starts in austenite grain boundary region, resulting in the high anisotropy of the microstructure [10]. High temperature annealing results in relatively thick and distinct grain boundaries along with the low dislocation density inside the submicron grains (Figs. 3(f) and 5(a)). This could be attributed to the recovery process associated with the absorption of dislocations by grain boundaries [20].

It has been noticed that the recrystallised area of 30% CD

and annealed (900 ℃) sample is more than that of 10% CD and annealed (900 ℃) sample (Fig. 2(d) vis-à-vis Fig. 4(d)). In this context, H. S. Zurob et al [21] reported that the driving force for recrystallisation is the stored energy of deformation, often expressed as:

$$E_{sto} = \frac{1}{2}\rho\mu b^2 \quad (1)$$

Where E_{sto} is stored energy of deformation, ρ is the dislocation density, μ is the shear modulus of the matrix and *b* is the burgers vector. D. N. Lee [11] also reported in a model that the driving force for recrystallisation is assumed to be the stored energy and the maximum stress direction becomes the minimum elastic modulus direction on recrystallisation. Hence, it is obvious that samples with higher deformation (30%) are more responsible for recrystallisation during annealing. It has been reported in literature [22] that the velocity (v) of grain boundary and in turn growth rate (G) of recrystallised grain is given by:

$$v = G = MP \quad (2)$$

Where M is the boundary mobility and P is the net pressure on the boundary. If the net pressure is divided in two parts – (i) driving pressure (P_d) and (ii) retarding pressure (P_c), then according to Gibbs-Thomson relationship, the retarding pressure on the grain boundary is depicted by:

$$P_c = \frac{2\gamma_b}{R} \quad (3)$$

Where R is the new grain radius; γ_b is the specific energy or grain boundary energy. In this literature [22], it has also been predicted that if the grain size is 2 μm (R = 1 μm) or less then there would be no net driving force for recrystallisation. So for very fine grain (twinned grain) there may be very low driving force for recrystallisation.

On the other hand, grain boundary specific energy is denoted by:

$$\gamma_b = \frac{dG}{dA} \quad (4)$$

Where γ_b is inversely proportional to grain boundary area, dA, i.e., if grain boundary area is large, then the surface energy will be low. In an earlier report [23], it has been seen that twins result in grain refinement by dividing the original grain into twin-matrix lamellae. So the driving force of twin free grain is high than a twinned grain for recrystallisation. The pressure as well as boundary velocity (v) may not be constant during recrystallisation. Therefore, the growth rate of recrystallisation is also a complex function of the material during annealing.

Based on the chemical composition of the present steel, the SFE has been estimated by thermodynamic calculations [24] to be as 24 mJ/m^2 and this low SFE plays an important role in recrystallisation. During annealing below 900 ℃, rearrangement of defect structures (dislocation annihilation, formation of dislocation cells etc.) takes place in order to reduce the strain generated during cold rolling. Dislocation dissociation is usually sluggish in low SFE materials. However, it is not only dependent on SFE, but also depends on temperature as well as amount of deformation where thermally activated restoration processes such as dislocation climb occurs during deformation. According to L. Bracke et al [25], twins remain after annealing at 580 ℃ because of the sluggish recrystallisation rate [13] of Fe–22Mn TWIP steel with low SFE. Wang et al [26] reported earlier that the thermal stability of the cold-deformed microstructure was examined by performing isochronal annealing experiments for 1 h at temperatures between 400°C and 800 ℃ for Fe–30Mn–0.5C steel.

According to B. Radhakrishnan et al [27], the growth velocity of a recrystallisation, G, can be expressed as

$$G = kF \quad (5)$$

Where k is the boundary mobility and F is the driving force. During recrystallisation, the velocity can increase or decrease if the boundary mobility and/or the driving force increase or decrease. The recrystallisation velocity depends on the boundary mobility. The boundary mobility is restricted by twins which is also an important reason for slow growth velocity during recrystallisation. The driving force increases as the prior cold work is increased. A. F. Padilha et al [28] observed for austenitic stainless steel, deformation twinning is also dependent on SFE and low SFE favours deformation twinning. However, different alloying concepts with similar SFEs result in different recrystallisation rate. In agreement with an earlier report [29], it may be mentioned that the twin boundary has a lower driving force than grain boundary during recrystallisation which results in thermal stability of twins. In this context, it is reasonable to conclude that as long as cold deformation is induced, the existence of mechanical twin is possible. A comparison with the earlier published results [30] indicates that there is no significant difference in the appearance of mechanical twins with those twins remaining after annealing at 900 ℃ (Figs. 3(d) and 5(d)).

It has been noticed that microstructural evolution indicating recovery at 600-800 ℃ and partial recrystallisation [31] at 900 ℃ can be confirmed by hardness evaluation (Fig. 7). During annealing, lowering in hardness and strength with the increase in ductility are more significant (Table 3 and Fig. 7) due to the possible lowering of dislocation density and associated strain. It is interesting to note that within the chosen range of annealing temperature, strengthening of material is mainly controlled by mechanical twins. Such type of twins which are originated from the austenite grain boundaries (Fig. 3(c)) [32] act as major obstacles for dislocation gliding [33]. It is also obvious that there is no evidence of twin growth even at 900 ℃ which is in good agreement with the earlier report [21].

Table 4. Mechanical properties of some of the advanced automotive steels

Processing/steel	HV	YS (MPa)	UTS (MPa)	TEL (%)
DP steel [35-37] [C, 0.09–0.21; Si, 0.03–2.48; Mn, 0.26–2.05 (wt%)]	160 - 300	265 - 620	465 - 984	11 - 42
TRIP steel [38, 39] [C, 0.1; Si, 0.12; Mn, 5.18–7.09 (wt-%)]	240–440	525–900	750–1400	6 - 40
Multiphase steel(Q&P) [40] 0.19C, 1.61Mn, 0.35Si, 1.1Al,	180	504	969	24

The newly formed partially recrystallised submicron austenite grains through nucleation and growth mechanism lead to a relatively high ductility. According to G. Dini et al [18], the presence of submicron grains in the partially recrystallised microstructure is probably due to a high density of accumulated dislocations during cold rolling which results in limited dynamic recovery in TWIP steel with low SFE. Wang et al [34] reported that a mixture of both ultrafine and fine grains may be also effective in achieving the best mechanical property of the steel. It is obvious that the decrease in hardness of 30% CD sample is more prominent than that of 10% CD sample at 800 ℃. Dislocation annihilation plays a much important role than recrystallisation on the decrease of hardness during this temperature. It appears that cold rolling and annealing treatment is the effective method to obtain submicron grain (Fig. 5(a)) in deformed TWIP steel with an excellent combination of strength and ductility (tensile toughness).

Table 4 represents hardness and tensile results of some of the advanced automotive steels. It is also interesting to note that the investigated hot rolled, cold rolled and cold rolled plus annealed steels are comparable with the DP, TRIP and multiphase steels (Table 3 vis-à-vis Table 4). Moreover, the current steel has yielded a significantly higher level of strength as compared to the conventional AHSSs at a much lower level of carbon (0.06 wt%). Usually cold rolled steel having large residual stress exhibits premature failure with low ductility. However, the residual stress is expected to be relieved during annealing at 600°C which is reflected in good combination of strength and ductility (Table 3). It is noteworthy that different cold rolling reductions and more annealing schedules are required for detailed observation in this regard.

5. Conclusions

Based on the above results, the major conclusions can be derived as follows:

1. Optical and TEM micrographs of 10% and 30% cold deformed samples exhibit dislocations, micro-shear bands, nano-scale (<100 nm) deformation twins as well as interaction of dislocations and twins. 30% cold deformed sample reveals higher amount of deformation twins than those of 10% cold deformed specimen.
2. Microstructural examination of cold deformed samples revealed recovery during annealing at 600 ℃ - 800 ℃ for 5 minutes. However, annealing at 900 ℃ showed partially recrystallised submicron grain with deformation twins.
3. The presence of deformation twin even at 900 ℃ indicates its thermal stability in the microstructure which could be related with the sluggish rate of recrystallisation due to relatively low SFE of about 24 mJ/m^2.
4. Hardness values dropped significantly from 244 HV to 169 HV and from 320 HV to 182 HV for10% and 30% cold deformed samples, respectively after annealing at 600-900 ℃.
5. Enhancement in ductility (34-48% for 10% and 29-43% for 30% cold rolled samples) and decrease in tensile strength (865-662 MPa for 10% and 926-812 MPa for 30% cold rolled samples) are achieved after annealing at 600 ℃.
6. 30% cold rolling and annealing is the effective method to obtain submicron grain with an attractive combination of strength and ductility.

ACKNOWLEDGEMENTS

The authors gratefully acknowledge the financial support provided by the Centre of Excellence (COE), TEQIP-II, IIEST, Shibpur, India for publication in the present journal.

REFERENCES

[1] A. Soulami, K. S. Choi, Y. F. Shen, W. N. Liu, X. Sun and M. A. Khaleel, *Mater. Sci. Eng. A*, Vol. 528, 2011, pp. 1402-1408.

[2] R. Ueji, N. Tsuchida, D. Terada, N. Tsuji, Y. Tanaka, A. Takemura and K. Kunishige, *Scr. Mater.*, Vol. 59, 2008, pp. 963-966.

[3] O. Grässel, L. Krüger, G. Frommeyer and L.W. Meyer, *Int. J. Plast.*, Vol. 16, 2000, pp. 1391–1409.

[4] D. Barbier, N. Gey, S. Allain, N. Bozzolo and M. Humbert, *Mater. Sci. Eng. A*, Vol. 500, 2009, pp. 196–206.

[5] G. Dini, R. Ueji, A. Najafizadeh and S. M. Monir-Vaghefi, *Mater. Sci. Eng. A*, Vol. 527, 2010, pp. 2759–2763.

[6] S. Allain, J. -P. Chateau and O. Bouaziz, *Mater. Sci. Eng. A*, Vol. 387-389, 2004, pp. 143-147.

[7] M. C. Somani, P. Juntunen, L. P. Karjalainen, R. D. K. Misra and A. Kyröläinen, *Metall. Mater. Trans. A*, Vol. 40, 2009, pp. 729-744.

[8] O. Bouaziz, C. P. Scott and G. Petitgand, *Scr. Mater.*, Vol. 60, 2009, pp. 714-716.

[9] V. Torabinejad, A. Zarei-Hanzaki, M. Sabet and H. R. Abedi, *Mater. Des.*, Vol. 32, 2011, pp. 2345-2349.

[10] Y. F. Shen, C. H. Qiu, L. Wang, X. Sun, X. M. Zhao and L. Zuo, *Mater. Sci. Eng. A*, Vol. 561, 2013, pp. 329-337.

[11] D. N. Lee, Scr. Metall. Mater., Vol. 32, 1995, pp.1689-1694.

[12] S. Vercammen, B. Blanpain, B. C. De Cooman and P. Wollants, *Acta Mater.*, Vol. 52, 2004, pp. 2005-2012.

[13] S. G. Chowdhury, S. Das, B. Ravikumar and P. K. De, *Metall. Mater. Trans. A*, Vol. 37 2006, pp. 2349-2359.

[14] N. K. Tewary, S. K. Ghosh, S. Bera, D. Chakrabarti and S. Chatterjee, *Mater. Sci. Eng. A*, Vol. 615, 2014, pp. 405-415.

[15] G. Dini, A. Najafizadeh, S. M. Monir-Vaghefi and R. Ueji, *J. Mater. Sci. Technol.*, Vol. 26, 2010, pp. 181-186.

[16] Y. Z. Tian, Y. Bai, M. C. Chen, A. Shibata, D. Terada and N. Tsuji, *Metall. Mater. Trans. A*, Vol. 45A, 2014, pp. 5300-5304.

[17] S.W. Thompson and P. R. Howell, *Mater. Sci. Technol.*, Vol 8, 1992, pp. 777-784.

[18] G. Dini, A. Najafizadeh, R. Ueji and S. M. Monir-Vaghefi, *Mater. Lett.*, Vol. 64, 2010, pp.15-18.

[19] D. B. Santos, A. A. Saleh, A. A. Gazder, A. Carman, D. M. Duarte, Érica A. S. Ribeiro, B. M. Gonzalez and E. V. Pereloma, *Mater. Sci. Eng. A*, Vol. 528, 2011, pp. 3545-3555.

[20] Kyung-Tae Park, Yong-Seog Kim, Jung Guk Lee and Dong Hyuk Shin, *Mater. Sci. Eng. A*, Vol. 293, 2000, pp.165-172.

[21] H. S. Zurob, C. R. Hutchinson, Y. Brechet and G. Purdy, *Acta Mater.*, Vol. 50, 2002, pp. 3077-3094.

[22] Humphreys FJ, Hatherly M. Recrystallisation and related annealing phenomena. 2nd ed. UK: Elsevier; 2004.

[23] K. Wang, N.R. Tao, G. Liu, J. Lu and K. Lu, *Acta. Mater.*, Vol. 54, 2006, pp. 5281-5291.

[24] A. Saeed-Akbari, J. Imlau, U. Prahl and W. Bleck, *Metall. Mater. Trans. A*, Vol. 40, No. 13, 2009, pp. 3076-3090.

[25] L. Bracke, K. Verbeken, L. Kestens and J. Penning, *Acta. Mater.*, Vol. 57, 2009, pp.1512-1524.

[26] X. Wang, H. S. Zurob, J. D. Embury, X. Ren and I. Yakubtsov, *Mater. Sci. Eng. A*, Vol. 527, 2010, pp. 3785–3791.

[27] B. Radhakrishnan, G. B. Sarma and T. Zacharia, *Acta. Mater.*, Vol. 46, 1998, pp. 4415-4433.

[28] A. F. Padilha, R. L. Plaut and P. R. Rios, *ISIJ Int.*, Vol. 43, 2003, pp. 135- 143.

[29] X. Zhang and A. Misra, *Scr. Mater.*, Vol. 66, 2012, pp. 860-865.

[30] C. Haase, S. G. Chowdhury, L. A. Barrales-Mora, D. A. Molodov and G. Gottstein, *Metall. Mater. Trans. A*, Vol. 44A, 2013, pp. 911-922.

[31] M. H. Razmpoosh, A. Zarei-Hanzaki, N. Haghdadi, Jae-Hyung Chob, Won Jae Kim and S. Heshmati-Manesh, *Mater. Sci. Eng. A*, Vol. 638, 2015, pp. 5-14.

[32] Jae-Eun Jin and Young-Kook Lee, *Mater. Sci. Eng. A*, Vol. 527, 2009, pp. 157-161.

[33] H. Idrissi, K. Renard, D. Schryvers and P. J. Jacques, *Scr. Mater.*, Vol. 63, 2010, pp. 961-964.

[34] Y. Wang, M. Chen, F. Zhou and E. Ma, *Nature*, Vol. 419, 2002, pp. 912-915.

[35] K. Sugimoto, J. Sakaguchi, T. Iida and T. Kashima, *ISIJ Int.*, Vol. 40, No. 9, 2000, pp. 920-926.

[36] M. H. Saleh and R. Priestner, *J. Mater. Process. Technol.*, Vol. 113, 2001, pp. 587-593.

[37] B. Mintz, *Int. Mater. Rev.*, Vol. 46, No. 4, 2001, pp. 169-197.

[38] M. J. Merwin, *Mater. Sci. Forum*, Vol. 539-543, 2007, pp. 4327-4332.

[39] M. J. Merwin, *Iron Steel Technol.*, Vol. 5, No. 10, 2008, pp. 66-84.

[40] I. de Diego-Calderón, M. J. Santofimia, J. M. Molina-Aldareguia, M. A. Monclús and I. Sabirov, *Mater. Sci. Eng. A*, Vol. 611, 2014, pp. 201-211.